

Z. RANACHOWSKI\*, D. JÓŹWIAK-NIEDŹWIEDZKA\*, P. RANACHOWSKI\*, F. REJMUND\*, M. DĄBROWSKI\*,  
S. KUDELA JR\*\*, T. DVORAK\*\*

## APPLICATION OF X-RAY MICROTOMOGRAPHY AND OPTICAL MICROSCOPY TO DETERMINE THE MICROSTRUCTURE OF CONCRETE PENETRATED BY CARBON DIOXIDE

### ZASTOSOWANIE MIKROTOMOGRAFII KOMPUTEROWEJ I MIKROSKOPII OPTYCZNEJ DO OCENY MIKROSTRUKTURY BETONÓW PODDANYCH DZIAŁANIU CO<sub>2</sub>

In the paper two advanced methods for testing cement based composites are described and compared. These are X-ray microtomography and optical microscopy. Microtomography supplies three-dimensional images of small concrete specimens. In the tomograms all cracks, pores and other voids and inclusions, that exceed a few micrometers, are shown. Such visualisation can become a valuable tool for analysis of the basic material properties. Images obtained on thin sections and analysed with various methods on optical microscopes supply additional information on material microstructure that cannot be obtained in tomograms. For example it is relatively easy to determine zone penetrated by CO<sub>2</sub> ingress. These two methods, presented on examples of tests, complete each another in order to supply a set of information on composition and defects of tested composite materials.

*Keywords:* cement matrix composites, concrete deterioration, X-ray tomography, microscopic analysis, concrete microstructure

W artykule przedstawiono dwie nowoczesne metody analizy struktury materiałów kompozytowych ze spoiwem na bazie cementu. Są to mikrotomografia komputerowa oraz optyczna analiza cienkich szlifów. Mikrotomografia pozwala na uzyskanie trójwymiarowych obrazów niewielkich próbek betonowych. Na tomogramach widoczne są układy rys, porów i innych pustek, których wymiary przekraczają kilka mikrometrów. Przetworzenie tych obiektów w przestrzeni jest ważnym narzędziem do analizy podstawowych właściwości materiału. Obrazy uzyskane na cienkich szlifach w mikroskopie optycznym, analizowane następnie różnymi metodami, dostarczają dodatkowych informacji o mikrostrukturze materiału, które nie mogą być dostrzeżone na tomogramach. Stosunkowo łatwo jest np. uzyskać obrazy stref skarbonatyzowanej matrycy cementowej. Obie przedstawione metody uzupełniają się wzajemnie i pozwalają na otrzymanie zbioru informacji o składzie i defektach badanych materiałów kompozytowych.

### 1. Introduction

The durability of concrete in civil engineering structures is closely related to its resistance to the aggressive environmental conditions, including air with oxygen, nitrogen, carbon dioxide as well as water with solutions of sulphates and chlorides. The above-mentioned media influence all concrete components but on the first place – concrete matrix and its microstructure. The evolution of the concrete microstructure under environmental aggression includes on the first place carbonation, that can cause serious reduction of durability of concrete works. Some aspects of the concrete microstructure degradation was discussed in the articles [1][2][17].

Modern technique of investigation of the concrete structures includes high resolution visualization with images that enable determination of existing microstructure with pores in the matrix. The pore system and pore interconnectivity direct-

ly influences penetration of CO<sub>2</sub> into concrete structure. The present possibilities of the image processing systems, with resolution of a few micrometers, are not capable to identify single crystallites or gel pores [3]. However, it is possible to investigate the most important elements of the microstructure, namely capillary pores system, pores voids and microcracks. It is also possible to determine the volumetric percentage of pores filled by various solutions and, to some extent, to determine the type of these solutions.

In the paper the results of two new methods of microstructural investigation are presented. In both digital image processing is applied. These methods are X-ray microtomography (micro-CT) and optical microscopy on thin sections of concrete. The microstructure of concrete matrix with high calcium fly ash content was the subject of presented investigation. Its aim was to determine the influence of aggressive gaseous media on the resistance to carbonation of the matrix. The

\* INSTITUTE OF FUNDAMENTAL TECHNOLOGICAL RESEARCH POLISH ACADEMY OF SCIENCES, 5B PAWIŃSKIEGO STR., 02-106 WARSZAWA, POLAND

\*\* INSTITUTE OF MATERIALS AND MACHINE MECHANICS SLOVAK ACADEMY OF SCIENCES, 75 RACIANSKA STR., 831-02 BRATISLAVA, SLOVAK REPUBLIC

advantages of these methods are remarkably improved when applied together, since it enables more complex and complete material characterization.

## 2. Application of X-ray microtomography for investigation of cement matrix composites

The tools for material testing with micro-CT technique are produced at present by a few manufacturers. They are capable to perform tests either on the small specimens – of some millimeter dimensions – either on extending to some meters. They include the microfocal source of X-ray radiation, the movable table to place a specimen, and the flat panel with a radiation detector, which resolution usually equals 2000 x 2000 pixels. The structure of concrete is visualized on the cross-sections (tomograms) of the investigated specimen. There is used grey scale convention, related directly to the amount of local radiation absorption of the material. The grey scale includes some tens of the levels and extends from the white colour – corresponding to maximum of absorption, towards the black colour – related with the minimum, respectively.

Unhydrated cement particles and aggregate grains are the objects of the greatest absorption. The hydration products, that cover major part of the cement matrix, present slightly lower absorption ability. The next in turn are hydrated calcinates and at the end of the scale are the regions of high porosity. The image resolution of tomograms is usually approximately ten times lower than that obtained in the thin sections (1  $\mu\text{m}$  resolution). However, application of micro-CT technique makes it possible to reconstruct a real 3-dimensional image of investigated microobjects and to determine the volumetric part of the material occupied by bulk matrix, aggregates, voids, pores, cracks, etc. In some cases it is also possible to improve the image resolution, such as in studies of Gallucci *et al.* [4].

A specimen for micro-CT testing should be extracted from the investigated concrete by drilling out a core with diameter about 12 mm. The testing procedure lasts about 30 minutes and does not require a special processing of the material surface. Therefore the method is especially useful to deliver quick, however not particularly precise microstructural parameters of the investigated material – e.g. for comparative analysis. Since the flat panel detectors usually represent the resolution of 2000 x 2000 pixels, it may be concluded that the effective image resolution is one promille of the greater specimen dimension. That is why the specimen dimensions cannot exceed a few millimeters. However, digitizing of the images of the microstructure enables merging the data obtained from several specimens into one set of data. The limitation of dimensions is the argument to limit to the matrix without coarse aggregate grains.

Slate and Olsefski [5] were the first researchers who applied the X-ray radiographic method in order to visualize the crack growth in compressed concrete specimens. They presented the radiograms of 100 micrometers resolution with visible only large cracks, aggregate grains and matrix.

Landis *et al.* [6] carried on compression tests of small mortar cylinders of 4 mm of diameter and of 12 mm of

height. The microtomograms were realized with application of high-energy synchrotrone source and recorded using CCD matrix of 512 x 512 pixels. One pixel of the obtained pictures represented the area of diameter equal 13.5  $\mu\text{m}$ . Within this range of stress no cracks were discovered. During the next experiments, in the compressed specimens the process of material decohesion was registered. Rapid onset of the system of cracks was registered after exceeding the critical load in the tested mortar. On the basis of a qualitative analysis of the test results the authors concluded that the area most affected by cracks appeared in the mortar of low density. When the loading of the specimen was increased the cracks extended in the mortar around fine sand grains and finally connected to one another. The applied method of testing allowed to trace the crack growth in all directions and to recognize the image of the entire crack system in the specimen.

Neither Slate and Olsefski [5] nor Landis *et al.* [6] had a software capabilities to evaluate the cracks lengths or the total volumetric concentration of pores. Therefore, the conclusions were restricted to the qualitative assesment of the recorded structure evolution during the crack growth process.

Lanzón *et al.* [7] used the micro-CT method to test the specimens made with crushed limestone aggregate (82.80 wt.%), cement CEM II/B-L 42.5R (16.50 wt.%) and additions (0.60 wt.%). The 0.1 wt. % of plasticizer was added to the prepared mixes. There were used three low-density mineral additions, significantly differed in their granulometric features – i.e. in mean and span of grain diameter distribution. These additions were: expanded perlite, expanded glass and cenospheres (hollow microspheres). The scanning was performed on cylinders with a diameter of 8 millimeters and a height of 8 millimeters, cut out from the bulk of the mortars. The resolution of 8  $\mu\text{m}$  per pixel was achieved in resulting tomograms. The authors determined capillary water absorption for mortars with the three different low density additions and for the reference mortar by partial immersion of the samples in water. The results agreed with the volumetric pore concentration data, obtained by processing of test results using micro-CT. The correlation coefficient of 0.964 was obtained between the air pores content determined using micro-CT and the capillary water absorption. The authors stated that nature of the mortars allows precise segregation of the air pores – since the air is clearly differentiated from the solid and gelled components.

Provis *et al.* [8] tested the mixtures of cement and siliceous fly ash as well as ground granulated blast furnace slag in different proportions after the ageing period of 4, 8, 16 and 48 days. The scanning was performed on the agglomerates of dimensions approx. 1 x 1 x 1 millimeter, with application of high-energy synchrotron source. Due to the use of high resolution detector a resolution of 0.75  $\mu\text{m}$  at the tomograms was achieved. The aim of investigation was to trace the volume evolution of pores and to determine the time changes of connectivity within the pore system. To characterise the connectivity of pores a diffusive tortuosity  $\tau_D$  was determined. The latter parameter is constructed on the basis of the paths created by movements of migrating abstract particles, called ‘walkers’, moving across the channels in the bulk of investigated material. It can be defined as the ratio of the paths length of a walker migrating due to diffusion across the free space to the

paths length of a walker migrating across the system of voids in the specimen. The authors revealed that the pore volume decreases in linear proportion to the sample hardening time in all investigated compositions. The decrease of pore volume was accompanied by the increase of their tortuosity. The parameters that characterize pores configuration can be applied as a measure of a susceptibility of cement binders to migration processes of aggressive media causing structural damages.

### 3. Application of optical microscopy and observations of thin sections

Optical microscopy is often applied as a supplementary method in testing the microstructure of the cement matrix composite. It is now possible to improve images from optical microscope observations of thin sections by adding a fluorescent feature and plane polarized and crossed polarized light techniques – Brandt and Józwiak-Niedźwiedzka [1], Józwiak-Niedźwiedzka *et. al.* [3][17].

The fluorescent illumination light gives information about the quality of aggregates and paste, air void system, structural defects, crack pattern and about the water to binder ratio. The obtained information is a valuable tool for identification of the deterioration processes developed in concrete, Józwiak-Niedźwiedzka and Tucholski [9]. Comparing to such methods as SEM, X-ray Diffraction Analysis and Differential Scanning Calorimetry, the advantage of using an optical microscope in concrete examination is that it offers larger field of view. However SEM, XDA and DSC are capable to supply more detailed set of information what leads to better recognition of deterioration mechanisms.

Pavia and Caro [10] applied the thin sections method for investigation of 26 specimens of Roman mortars, used in the period of 1500÷2000 years ago. This method enabled to perform the petrographic analysis of collected material and to reconstruct the ancient technologies of production of cement paste as well as firing and slaking of lime.

Jakobsen and Brown [11] determined water to cement (w/c) ratio in concretes with an accuracy of ±0.02 on the basis of the brightness of thin sections under fluorescent light. Fernandes *et al.* [12], Georgali and Tsakiridis [13] applied thin sections technique to determine the cause of concrete deterioration, influenced by such factors as acid corrosion and elevated temperature action.

The drawbacks of the optical microscopy include the limitation of the image resolution to single micrometers. It is caused by the relative long wavelength of a visible light and the requirements of minimum energy amount necessary to trigger the image sensor. Application of micro-CT method enables the use of more powerful sources of light with wavelengths shorter in two orders of magnitude. Then imaging of the entire specimen volume is possible. This is considered to be a remarkable improvement in comparison to the two-dimensional images, obtained using transmission optical microscopy.

### 4. Experimental program

The reference concrete mix was designed and prepared in a way to comply with the requirements of XC3 environmental exposition class (carbonation) [14]. The reference specimens, designated PW-0, contained 0% of fly ash and the other mixtures – 30% replacement of cement mass by high calcium fly ash (HCFA). Design of the fly ash concrete mixtures did not take into consideration the PN-EN 206-1 [14] requirements in relation to *k*-value and maximum content of the fly ash treated as type II addition. The presented results constitute a part of the larger research project, concerning concretes with addition of HCFA and neglected *k*-value – Gibas and Glinicki [15]. The chemical composition of the high calcium fly ash used in the research is presented in Table 1.

Two kinds of HCFA were used:

- as delivered and unprocessed, mixture designated PW-NM-30;
- after passing through 0.045 mm sieve – removed larger fraction, mixture designated PW-45-30.

HCFA was subjected to sieving in order to increase its grain specific surface and to remove unburned coal particles. The processed fly ash was characterized by specific density of 2.67 g/cm<sup>3</sup>, Blaine specific surface 3520 cm<sup>2</sup>/g and fineness 20.8%. The mixes were designed with the same water to binder ratio of 0.55. Identical consistency was achieved by adding the proper amount of plasticizer. The addition of polycarboxylane ether was used only to the mixes containing unprocessed fly ash. It was observed that the removal of the grain fractions above 45 μm improved the workability of the concrete mix.

TABLE 1

Chemical composition of the high calcium fly ash, XRF method, [%]

LOI	SiO <sub>2</sub>	Al <sub>2</sub> O <sub>3</sub>	Fe <sub>2</sub> O <sub>3</sub>	CaO	MgO	SO <sub>3</sub>	K <sub>2</sub> O	Na <sub>2</sub> O	P <sub>2</sub> O <sub>5</sub>	TiO <sub>2</sub>	CaO <sub>w</sub>
2.12	40.9	19.0	4.3	26.0	1.7	3.9	0.14	0.13	0.1	1.5	1.07

TABLE 2

Composition of tested concretes, kg/m<sup>3</sup>

Concrete designation	CEM I 42.5R	HCFA	Fine aggregates, 0÷2 mm	Coarse aggregates, 2÷8 mm	Coarse aggregates, 8÷16 mm	Water	Super-plasticizer, wt%
PW-0	320	0	630	675	650	176	0.00
PW-NM-30	224	96	630	675	650	176	0.10
PW-45-30	224	96	630	675	650	176	0.00

The less agglomerates containing the unburned coal particles remains in the prepared concrete mixture, the better is workability of the prepared mixes. Sand of fraction 0÷2 mm was used as a fine aggregates and crushed amphibolite of fractions 2÷8 and 8÷16 mm was used as a coarse aggregates. The composition of concrete mixtures is shown in Table 2.

The beams with dimensions of 100 x 100 x 500 mm were cast for testing of progress of carbonation and stored for 27 days in water at temperature of +22°C. Then they were stored at laboratory conditions at +20°C and a relative humidity of 60% – until their mass equilibrium was reached – 14 days. The carbonation test was carried out at constant concentration of CO<sub>2</sub> of 1%, at the temperature of +22°C and relative humidity of 60%. After 0, 28 and 56 days the carbonation depth was determined on the freshly broken specimens surface. It was treated by 1% dilution of phenolphthalein, dissolved in 70% water solution of ethyl alcohol, in accordance with the standard PN-EN13295:2005, [16]. The mean value of a few results of measurements was determined.

The reference concrete made with Portland Cement without any addition of high calcium fly ash showed the highest resistance to carbonation after 56 days of exposure to 1% CO<sub>2</sub> atmosphere. Lower resistance was obtained for both concretes with 30% addition of HCFA – sieved and unprocessed – Table 3.

TABLE 3

Penetration depth of CO<sub>2</sub> after 0, 14, 28 and 56 days of exposure to 1% CO<sub>2</sub>

Concrete designation	Number of days			
	0	14	28	56
PW-0 (reference)	0	4.7	4.9	7.3
PW-NM-30 (unprocessed HCFA)	0	6.1	7.7	9.1
PW-45-30 (sieved HCFA)	0	5.6	7.6	8.6

## 5. Microstructure experimental methods

Micro-CT method was applied using Nanotom 30 microtomograph made by General Electric operating in the Institute of Materials and Machine Mechanics SAS in Bratislava. The equipment was capable to produce the following three different data sets depicting the specimen microstructure:

1 – digital specimen images representing cross-sections of investigated object in transverse or parallel direction to the main axis of the cylindrical sample;

2 – lists of all pores detected in the specimen volume with specification of their coordinates, equivalent diameters and surfaces;

3 – three-dimensional projections of specimens with marked local void concentrations presented by means of colour mappings.

Tomography analysis is performed usually on the specimens made of pastes or mortars [4] [5] [6] [7] [8], but in this research the cores were drilled out from concrete specimens submitted accelerated carbonation test. The drilled cores were prepared in such a way to avoid the presence of

coarse aggregate. Such small core dimensions arose due to required resolution and limitation of the used apparatus. The core dimensions were chosen in order to perform the procedure of micro-CT scanning. The space resolution of the reconstructed microstructure was 10 μm per voxel. Voxel is a three-dimensional equivalent of a pixel used to characterize two-dimensional digital images. In Fig. 1 is presented the view of the tested cores.

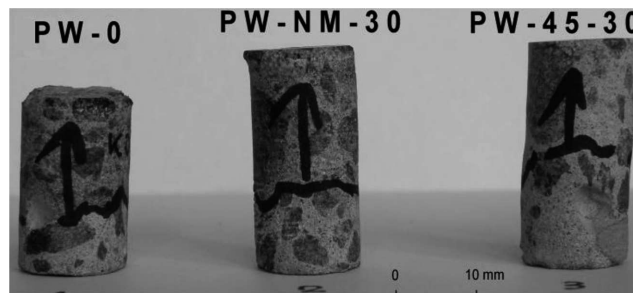


Fig. 1. Cores of 12 mm of diameter, cut out from the tested specimen

The result of micro-CT scanning was a set of tomograms (specimen cross-sections), performed every 100 μm along the specimen height. The digitized dataset of the first type characterized the consecutive cross-sections of the specimen and included the information about the material brightness in arbitrary units [a.u.], for all pixels at specimen surface. It was proportional to the local density of the material. After review of the brightness of a large set of tomograms, it was concluded that the magnitudes of brightness were depicted in the images in following manner: the area of voids 19÷40 [a.u.]; the cement paste (binder) area 41÷100 [a.u.] and the aggregates 101÷255 [a.u.]. The digitized dataset of the second type characterized the population of pores detected in the specimen using special algorithm, which was capable to recognize pores within the effective diameter range of 30÷1000 μm. The pores ranged from 30 to 100 μm contributed only to a part of total matrix porosity. Capillary porosity was not taken into consideration. Except coordinates, estimated diameter and surface of the void, collected data included calculated precision of the estimation.

Thin sections were separated from specimens after 56 days of carbonation process and were cut out in such a way to enable analysis of both - carbonated and uncarbonated concrete regions. The material was impregnated by epoxy resin and processed according to the procedure reported in Józwiak-Niedźwiedzka and Tucholski [9]. The observations were performed using plane polarized and crossed polarized light as well as fluorescent facility with application of an optical stereomicroscope.

## 6. Experimental results

### 6.1. Results of micro-ct tests

In order to examine local variations of the mortar density in the specimens an analysis of the micro-CT dataset no 1, described with information on brightness of pixels constituting the tomograms, was performed. Considering the significant differences of brightness representing voids, mortar and aggregates it was possible to separate various mortar regions –

Fig. 2. Mentioned above procedure enabled also comparison of average density of the matrix of three investigated specimens, prepared from the mixtures having different composition – Fig. 3.

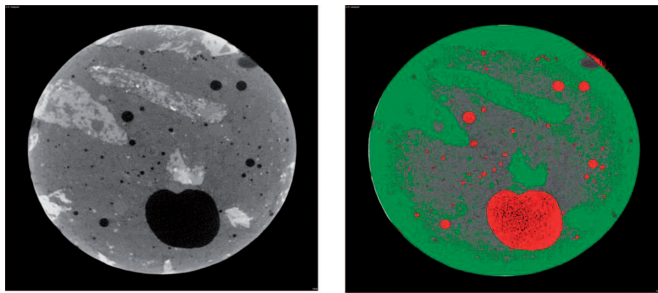


Fig. 2. Procedure of the area classification to the matrix region excluding aggregates and air pores. At the left – the microtomogram before processing. Composite matrix, aggregates and air pores are presented in a grey scale. At the right – microtomogram after processing. Matrix areas are marked grey, air pores – marked red, aggregate grains are green; diameter 12 mm

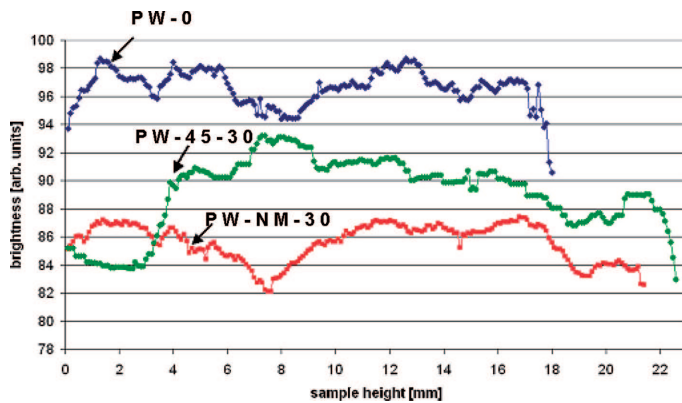


Fig. 3. Comparison of the averaged brightness of three investigated samples as a function of specimen height. The higher brightness is proportional to higher density of the concrete matrix. Designation of the samples as in Table 1

The comparison of the averaged brightness of three investigated specimens allow to conclude that the mortar labelled PW-0 with no HCFA represents the highest density. On the contrary, the lowest density mortar is that containing unprocessed HCFA. In Fig. 3 are visible local sharp brightness changes. They are caused by the presence of cracks and structural damages, mostly at the both specimen edges.

The analysis of digital data characterising voids - mostly air pores - detected in specimen volume, with specification of their coordinates, enabled to determine some parameters related to the amount and distribution of pores in the investigated specimens. These parameters, determined for the voids with the diameter in the range of 30÷3000 μm, are collected in Table 4.

On the basis of the data presented in Table 3 it can be concluded that the specimen without HCFA replacement of cement was characterised by significantly higher volumetric concentration of air pores than in case of both concretes with addition of HCFA. There is a considerable difference in number of pores in two latter composites caused by the difference in implemented HCFA grain fineness. It is the evidence

of the different pore diameter distribution in the specimens PW-NM-30 and PW-NM-45-30. The latter statement is illustrated by the volumetric pore diameter distribution of three investigated specimens, presented in Fig. 4.

TABLE 4

Parameters related to the porosity of the tested specimens, determined on the basis of the digital data describing the pores detected in the specimens

Material parameter	Specimen PW-0	Specimen PW-NM-30	Specimen PW-45-30
Volumetric concentration of air voids	1.71%	0.48%	0.44%
Average distance between the voids	194 μm	193 μm	121 μm
Total amount of voids	18183	6185	17901

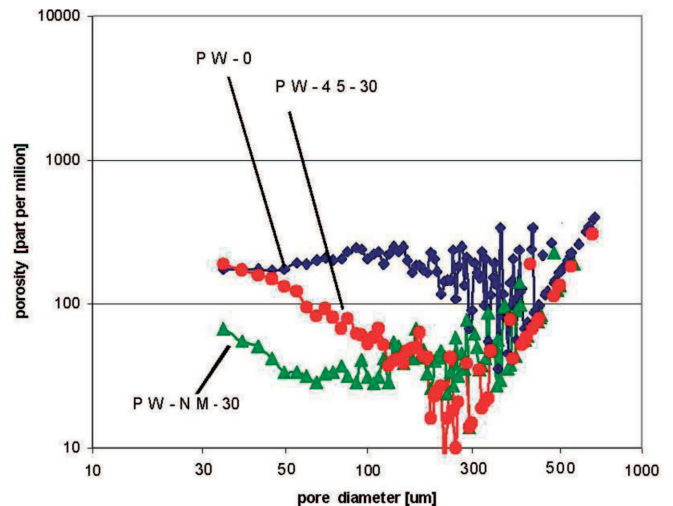


Fig. 4. Volumetric pore diameter distribution of the three tested specimens

The results presented in Fig. 3 reveal that in the specimen with no HCFA addition there is more pores of diameter above 80 μm than in the other two specimens made with addition of HCFA. It is also clearly visible that in the specimen PW-45-30 with finer - sieved HCFA grains there is more pores of diameter below 100 μm than in PW-NM-30 specimen. Instead the last sample contains more bigger voids – above 100 μm. The concentration of pores above 300 μm is for the three specimens indistinguishable, since it is not connected with the presence of ash in the samples structure. The diameter of HCFA grains is lower than 300 μm.

High volumetric ratio and nonuniform distribution of air voids and cracks in tested specimens make the task of determination of local voids concentration as a function of sample depth a complex problem. The phenolftalein test revealed the presence of carbonation variations in upper parts of all specimens presented in Fig. 1. The method of micro-CT was not capable to distinguish the changes of material density caused by carbonation.

### 6.2. Results of optical tests

There were no microstructural modifications due to carbonation observed with phenolphthalein method before testing, so the thin sections were extracted from the specimens exposed for 56 days to 1% CO<sub>2</sub> atmosphere and analyzed using optical microscope and transmission light technique.

The microscopic analysis of thin sections confirmed the depth of CO<sub>2</sub> penetration and the clear difference between the outer carbonated layer and the inner regions was visible. The carbonation front was placed at the same distance from the specimen surface along the entire broken surface. The local presence of aggregate grains did not influence the CO<sub>2</sub> penetration depth into the matrix. The differences in carbonated and uncarbonated mortar, shown in transmission and crossed polarized light, are shown in Fig. 5. There are visible multi-coloured portlandite particles in the uncarbonated area at the left side and labelled (a). Instead – fine pink particles of calcite in a larger amount, situated in the carbonated area are visible at the right side, labelled (b).

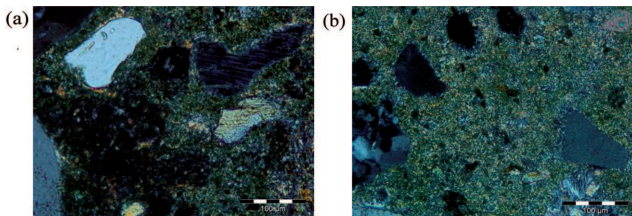


Fig. 5. Microstructure of concrete without HCFA. (a) – uncarbonated paste; (b) – carbonated paste; both structures prepared after 56 days of exposure to 1% CO<sub>2</sub>; thin sections projected in transmission and crossed polarized light, magnification of 200x

An example of microslides from optical microscope is shown in Fig. 6, projected in transmission light of reference concrete and of concretes with two types of fly ash. In the concrete without HCFA a few partly hydrated alite grains with characteristic transition zones around them are shown. The grains are uniformly dispersed in the entire image.

In both concretes with addition of fly ash, spherical ash grains are present. The size of these grains decreases as a result of elimination by sieving the unburned coal grains. The difference in the microscopic images of the matrix obtained using two types of fly ash addition (as received and sieved) is clearly seen.

The analysis of thin sections of the investigated concretes revealed that the maximum size of unburned coal grains in unprocessed fly ash was approximately 200 μm. After sieving process the size of these grains fell to below 43 μm. The mean size of unburned coal grains in unprocessed fly ash was in the range of 120 ÷ 140 μm. In sieved HCFA, with grains below 45 μm, the size of unburned coal particles decreased five times - when compared with unprocessed fly ash – and was in the range of 15 ÷ 30 μm, respectively. The procedure of ash grains sieving appeared to be effective and resulted in large decrease of their size. Additionally, the latter effect caused more homogenous grain dispersion in the fresh mixture and therefore homogenous distribution of the ash grains in the mortar.

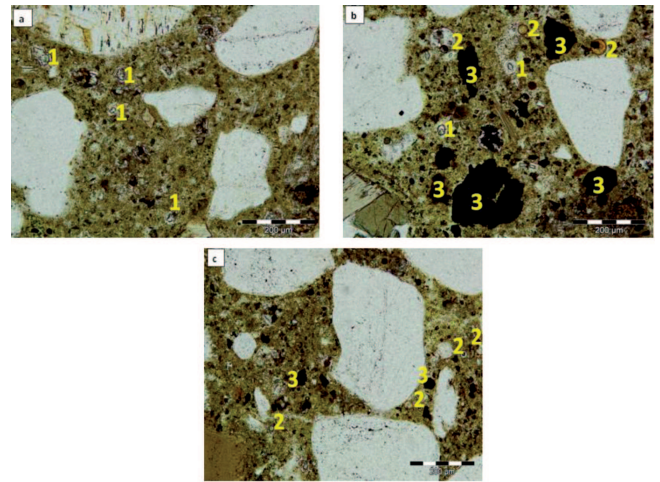


Fig. 6. Microstructure of concrete observed after 56 days of exposure to 1% CO<sub>2</sub>. Thin sections projected in transmission and plane polarized light: (a) - without HCFA addition; (b) – 30% of unprocessed HCFA addition; (c) – 30% of HCFA content, sieved grains above 45 μm. There are marked: 1 – alite grain, 2 – spherical fly ash grain, 3 – unburned coal grain

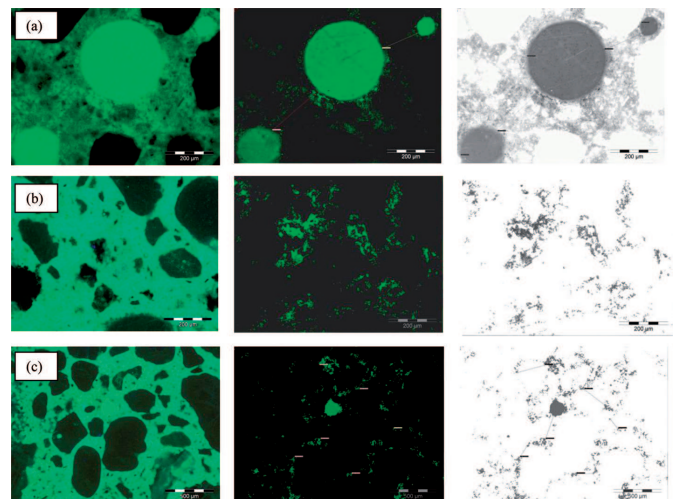


Fig. 7. The images of microstructure of investigated concretes obtained with application of thin sections and fluorescent light micrography – left column. The same images after image processing – middle and right column. (a) – concrete without HCFA addition; (b) – concrete with 30% of unprocessed HCFA addition; (c) – concrete containing 30% of HCFA, sieved grains above 45 μm. Description in the text

In Fig. 7 are presented the images of microstructure of the investigated concretes, obtained with application of fluorescent light micrography. The vertical columns show the consecutive stages of their digital processing, consisting of contrast increase and segmentation. The segmentation is an operation of transformation of coloured image first into a 256 stages grey scale image and finally into a black and white one. At the micrograph made in fluorescent light the porous matrix regions are presented as light green colour. The extraction of these regions and of air voids of the remaining concrete constituents is based on the analysis of the image colour histogram of all regions appearing in the micrograph. It is constructed for all the phases of the concrete, which can be distinguished on the basis of colour intensity. The colour histogram incorporates all colour intensity projections in order from the number 0 – assigned to the darkest region, to the number 255 – assigned

into the brightest region. Within such sequence a narrow segment of intensity was extracted and associated with the colour of porous regions. During the final step, all image pixels depicting the non-porous regions are converted to white and the porous regions are imaged as black colour.

The comparison of the processed micrograms allows to conclude that the addition of the HCFA resulted in a decrease of the amount of absorbed air bubbles into the fresh mixture, when compared to their amount in the reference concrete. The addition of sieved fly ash resulted in decrease of amount and size of these bubbles from about 400  $\mu\text{m}$  to approximately 150  $\mu\text{m}$  – regarding their parameters in unprocessed fly ash.

## 7. Conclusions

The results of the study, presented in this paper, indicate that the information on the microstructure of investigated materials, gained using optical microscopy and micro-CT complement one another. This can be used for further studies of the concrete structures. The microscopic analysis of thin sections of the concrete samples confirmed the range of carbonation, determined by phenolphthalein solution test. The presence of the coarse aggregates – such as crushed amphibolites – did not affect the diversity of carbonation range in the concrete matrix. The thin sections microscopic tests enabled a distinction of the specimen regions situated before and behind the carbonation front. The micrographs were useful to recognize HCFA grains and the particles of unburned coal. However, in the microtomograms these two kinds of particles cannot be distinguished from each other.

The micro-CT method was useful to assess the modifications of the concrete matrix density due to application of two kinds of HCFA – as received and after processing. The analysis of the digital data, characterizing the voids detected in specimens with specification of their coordinates and diameters, enabled to assess the parameters characterizing the specimens' porosity. Determination of the pore diameter distribution in the range from 30 to 1000  $\mu\text{m}$  was possible.

Replacement of 30% of the cement by unprocessed HCFA entailed loss of resistance to carbonation when comparing to the properties of the reference specimen of concrete. The results of the research did not allow to state if removal of the coarse fractions from the fly ash influenced positively to the resistance of the concrete to carbonation.

The reduction of the ash particle diameters by sieving caused the improved – i.e. more homogenous particles dispersion in the fresh mix and finally in the concrete matrix. The size of the spherical ash particles was reduced due to the operation of ash processing and because of lowered size of unburned coal particles.

It can be concluded that both applied test methods, including the phenolphthalein test, delivered important information on the microstructure of the concrete prepared with HCFA addition and exposed to  $\text{CO}_2$  action.

## Acknowledgements

The part of the results presented in the paper were obtained within the project “Innovative cement binders and concretes with ad-

dition of high calcium fly ash” (project no POIG.01.01.02-24-005/09 with the Polish Ministry of Science and Higher Education) in the framework of the Operational Programme Innovative Economy 2007-2013.

## REFERENCES

- [1] A.M. Brandt, D. Józwiak-Niedźwiedzka, Diagnosis of concrete quality by structural analysis, *Advances in Civil Engineering Materials* **1**, 1, 1-21 (2012).
- [2] Z. Ranachowski, D. Józwiak-Niedźwiedzka, A.M. Brandt, T. Dębowski, Application of acoustic emission method to determine critical stress in fibre reinforced mortar beams, *Archives of Acoustics* **37**, 3, 261-268 (2012).
- [3] D. Józwiak-Niedźwiedzka, A.M. Brandt, Z. Ranachowski, Self-healing of cracks in fibre reinforced mortar beams made with high calcium fly ash, *Cement, Lime, Concrete* **1**, 38-49 (2012).
- [4] E. Gallucci, K. Scrivener, A. Groso, M. Stambanoni, G. Margaritondo, Experimental investigation of the microstructure of cement pastes using synchrotron X-ray microtomography ( $\mu\text{-CT}$ ), *Cement & Concrete Research* **37**, 2007, 360-368 (2006).
- [5] F. Slate, S. Olsefski, X-ray study of internal structure and microcracking of concrete, *J. of American Concrete Institute* **60** (5), 575-588 (1963).
- [6] E. Landis, E. Nagy, D. Keane, S.P. Shah, Observations of internal crack growth in mortar using X-ray microtomography, *Proc. of the Fourth Materials Engineering Conf. Washington, D.C., ASCE. New York* (1996).
- [7] M. Lanzon, V. Cnudde, T. de Kock, J. Dewanklele, X-ray microtomography ( $\mu\text{-CT}$ ) to evaluate microstructure of mortars containing low density additions, *Cement & Concrete Composites* **34**, 993-1000 (2012).
- [8] J.L. Provis, R.J. Myers, C.E. White, X-ray microtomography shows pore structure and tortuosity in alkali-activated binders, *Cement & Concrete Research* **42**, 855-864 (2012).
- [9] D. Józwiak-Niedźwiedzka, Z. Tucholski, Reinforced concrete viaduct from beginning of the 20th century – microstructure analysis of 100 years old concrete, *Drogi i Mosty* **9**, 3, 23-37 (2010), (in Polish).
- [10] S. Pavia, S. Caro, An investigation of Roman mortar technology through the petrographic analysis of archaeological material, *Construction & Building Materials* **22**, 1807-1811 (2008).
- [11] U.H. Jakobsen, D.R. Brown, Reproducibility of w/c ratio determination from fluorescent impregnated thin sections, *Cement & Concrete Research* **36**, 1567-1573 (2006).
- [12] I. Fernandes, M. Pericão, P. Hagelia, F. Noronha, M.A. Ribeiro, J. Maia, Identification of acid attack on concrete of a sewage system, *Materials & Structures* **45**, 337-350 (2012).
- [13] B. Georgali, P.E. Tsakiridis, Microstructure of fire-damaged concrete. A case study, *Cement & Concrete Composites* **27**, 255-259 (2005).
- [14] PN-EN 206-1: 2003, Concrete – Part 1: Specification, performance, production and conformity.
- [15] K. Gibas, M.A. Glinicki, Influence of calcereous fly ash on concrete resistance to migration of chlorides, *Brittle Matrix Composites BMC-10*, 367-376 (2012).
- [16] PN-EN 13295: 2005, Products and systems for the protection and repair of concrete structures. Test methods. Determination of resistance to carbonation.
- [17] D. Józwiak-Niedźwiedzka, A.M. Brandt, K. Gibas, P. Denis, The alkali-aggregate reaction hazard in the case of barite concretes, *Cement, Lime, Concrete* **19**, 4, 234-242 (2014).